Journal Name

ARTICLE TYPE

Cite this: DOI: 00.0000/xxxxxxxxxx

Supplemental Materials: Waste heat recovery using thermally responsive ionic liquids through TiO2 nanopore and macroscopic membranes

Marc Pascual,[a‡] Nicolas Chapuis,[a‡] Soufiane Abdelghani-Idrissi,[a] Marie-Caroline Jullien,[b] Alessandro Siria,[a] and Lydéric Bocquet[a]

Received Date
Accepted Date

DOI: 00.0000/xxxxxxxxxx

1 Physico-chemical properties of the system

This first section gathers standard measurements made on the water-ionic liquid (IL) mixture of interest.

Fig. S1(a) displays the phase diagram of the water-IL mixture with the IL concentration on the horizontal axe (instead of the IL mass fraction used in Fig. 1(c) of the main text). For a separation temperature of 50^{o}C the concentration ratio of the two separated phases c_{max}/c_{min} is around 9.

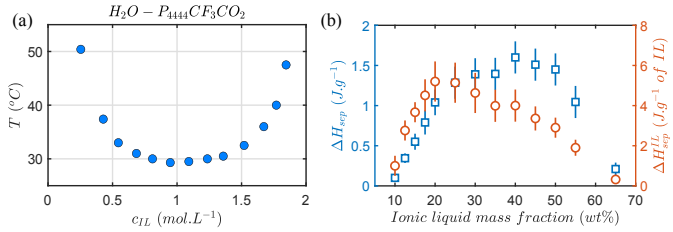

Fig. S 1 (a) Phase diagram of the water-IL mixture as a function of IL concentration. The critical point of this LCST system is at 35 wt% (0.95 M) in IL and 29.5^oC. (b) Latent heat absorbed by the mixture upon separation, measured by DSC technique.

The latent heat of separation for the $P_{4444}CF_3CO_2 - H_2O$ mixture has been measured for different concentration by differential scanning calorimetry (DSC - *TA instruments Q*20). The latent heat per gram of binary mixture is plotted as blue squares on Fig. S1(b). It shows a maximum around 35-40 wt% in ionic liquid, *i.e.* around the critical point of the mixture. We also plot the latent heat normalised by the mass of IL contained in the mixture as orange circles. We recall here that the latent heat (enthalpy) of phase separation measured here ≈ 2 J.g^{-1} is roughly three orders of magnitude lower than the latent heat of vaporization of a liquid-gas system: the LCST mixture requires less energy to be separated than distillation-based waste heat recovery techniques. This is relevant since the energy harvested on the salinity gradient is proportionnal to the entropy of mixing. However the distillation approach may lead to higher concentration ratio c_{max}/c_{min} after separation.

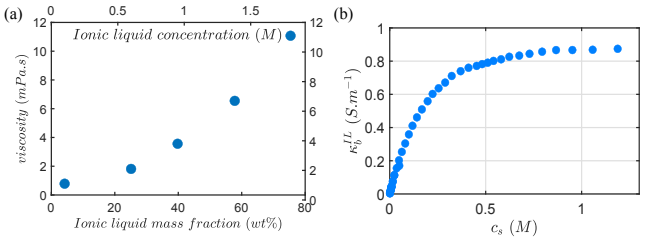

Fig. S 2 (a) Viscosity of the IL-water mixture as a function of IL mass fraction (bottom axis) and IL concentration (top axis), at 25^{o}C. (b) IL-water conductivity versus IL concentration.

Fig. S2(a) presents the viscosity of the binary mixture for five different concentrations, measured at 25^{o}C with a cone-and-plate geometry (*Anton-Paar MCR* 102). The viscosifying effect of the ionic liquid is to be considered if one wishes to minimize charge losses in the fluidic system.
The bulk conductivity of the system, measured with a conductimeter (*Hanna Instruments HI*2315), is shown on Fig. S2(b). It increases linearly with the salt concentration until 0.1 M, then it flattens and even decreases slightly at higher IL concentrations. This behavior can be linked to the weak electrolyte behavior of the ionic liquid, which is known to form aggregates above 0.1 M.

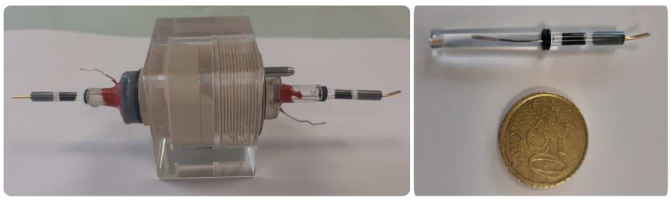

Fig. S 3 Photo of the fluidic cell with the two low profile reference electrodes inserted. On the right is presented one of these electrodes with a 0.50 euro coin for scale.

[a] *Laboratoire de Physique de l'Ecole Normale Supérieure, ENS, Universite PSL, CNRS, Sorbonne Université, F-75005 Paris, France*
[b] *Université Rennes 1, CNRS, IPR (Institut de Physique de Rennes) - UMR 6251, F-35000 Rennes, France*
‡ These authors contributed equally to this work

Fig. S3 shows on the left a picture of the homemade fluidic cell used for the measurements with the nanopores and on the right a close-up on a small reference electrode used in this study. The nanopore is sandwiched in the middle of the cell with two reservoirs of liquid on each side. In each reservoir is inserted a homemade Ag/AgCl electrode (shiny wire 0.5 mm thick) and a commercial Ag/AgCl reference electrode (60 mm long and 3.5 mm thick, *PineResearch - RRPEAGCL2*).
The homemade Ag/AgCl wires are used to impose a potential difference and collect the associated ionic currents. The commercial reference electrodes are used to screen the electrode potential of the homemade Ag/AgCl electrodes before and after each measurement.
Although we do not expect the ionic liquid to react faradically with Ag/AgCl electrodes in the $\pm$ 0.1 V window, the choice of Ag/AgCl instead of Pt electrodes is justified by the greater stability and reproducibility of their electrode potential.

2 Measurements with KCl for an individual nanopore

Once the nanopores have been coated with TiO_2 and annealed, conductance and diffusio-osmotic measurements are carried with KCl electrolyte before moving to IL-water mixtures in order to check the nanopores consistency.

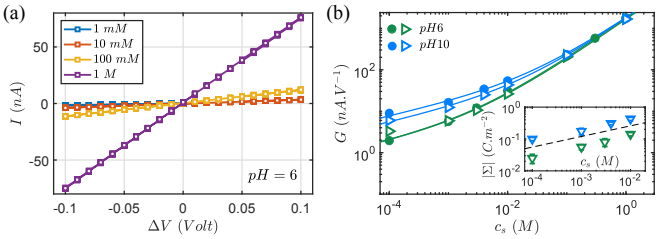

Fig. S 4 (a) Current versus voltage curves for an individual TiO_2 nanopore at different concentrations in KCl, pH 6. The pore length is 500 nm and its diameter is 200 nm. (b) Experimental conductance values for two TiO_2 nanopores (triangles and circles) filled with KCl at pH=6 (green) and 11 (blue). The solid lines are fits from equation 1 in main text. (inset) Surface charge Σ versus the salt concentration.

$I-V$ curves of a single TiO_2 nanopore filled with KCl at pH 6 are plotted on Fig. S4(a). The conductance values derived from the slope of theses curves are gathered on Fig. S4(b). As expected from a charged nanopore the conductance G shows a non-linear dependence at lower concentrations and the increase of G with the pH proves the pore negative charge. The inset on the bottom right shows the surface charge in $C.m^{-2}$ as a function of the concentration, deduced from the fit of the conductance curves using equation 1 in the main text. We recover a 1/3 slope which is caracteristic of the $\Sigma \sim c_s^{1/3}$ scaling.

We also check the diffusio-osmotic currents in the nanopore with different KCl concentration ratio. Fig. S5(a) shows an $I-V$ curve obtained with 0.003 M and 0.1 M in each reservoirs, at pH 11. The current shows a slight rectification and an offset of 19 nA at $\Delta V = 0$, this offset being the sum of the Nernst current (with $c_{max}/c_{min} = 33.3$ ratio the Nernst potential is $\approx 80\ mV$) and the diffusio-osmotic current I_{DO}.
The inset gives the electrode potential of the homemade Ag/AgCl wires immersed in each reservoir versus the Ag/AgCl saturated reference electrode during the experiment (we switch from closed to open circuit to perform this measure): we recover the expected values of 98 mV at 0.1 M and 180 mV at 0.003 M versus the Ag/AgCl reference electrode as predicted by the Nernst formula, yielding a Nernst potential across the nanopore of 82 mV here.
The substraction of the Nernst currents allows to isolate the diffusio-osmotic contribution I_{DO} to the current at $\Delta V = 0$, the former is plotted in Fig. S5(b). From equation 4 of the main text we can derive $I_{DO} \sim 2\pi R\Sigma D_{DO}\nabla c_{inf}/c_{inf}$. Knowing that with KCl salt we have $\Sigma = ac_s^{\gamma}$, we obtain:

$$I_{DO} \approx \frac{2\pi R D_{DO}}{\gamma L} a c_{max}^{\gamma}(1-(c_{min}/c_{max})^{\gamma}) \quad (1)$$

with $\gamma = 1/3$. We recover the $c_{max}^{1/3}$ scaling of the current and the increase with c_{max}/c_{min}.

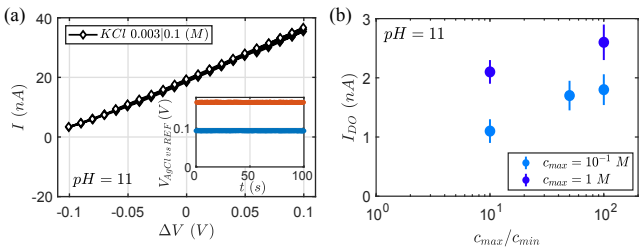

Fig. S 5 (a) I-V curve for a TiO_2 nanopore in a gradient of KCl at pH 11. (inset) $Ag/AgCl$ electrode potential versus the reference electrode, for both reservoirs (blue is 0.1 M; orange is 0.003 M). (b) Diffusio-osmotic current versus the concentration ratio c_{max}/c_{min} for a TiO_2 coated nanopore at pH 11.

Once such results have been obtained for a nanopore, it is rinsed with water and the measurements with IL electrolytes are performed (see Fig. 2-5 of the main text).

Another control experiment to probe the nanopore surface charge filled with KCl electrolyte is the streaming current measurement: under a pressure drop across the nanopore we record an ionic current induced by the net charge flow in the Debye layers. On Fig. S6(a) we see a linear increase of the streaming current I_{str} as a function of the pressure drop ΔP (dark squares).
In order to get a better understanding of the nanopore surface charge behavior when it is filled with IL solutions, the same measurements where conducted with the IL-water mixtures for a wide range of concentration and pH, see Fig. S6(a-c). Firstly, the streaming current sign does not change when pH varies from 4 to 12, indicating a steady negative surface charge in this pH range. Secondly, the current intensity first increases with the concentration then decreases at higher salinity; a classical behavior observed in streaming currents measurements. We conclude that no surface charge inversion occurs when the IL concentration is increased. The zeta potential ζ of the nanopore can be extracted from these data using the following relation:

$$I_{str} = \frac{\pi R^2 \zeta \varepsilon_0 \varepsilon}{\eta L} \Delta P \quad (2)$$

with R the pore radius, L the pore length, ε_0 the permittivity of vacuum, ε the relative permittivity of the liquid, η the viscosity and ΔP the pressure drop applied. The dependence of ζ on the salt concentration is plotted on Fig. 3(a) in the main text.

3 Characterisation of TiO2 membrane and measurement with KCl

The macroscopic TiO_2 membrane from Fraunhofer IKTS consists of an asymmetric structure. The support (thickness of 1 mm) gathers several intermediate porous layers made on TiO_2 with tortuous pores of $5\mu m$ in average size. These large grains can be seen in the lower part of Fig. S7(d))
We characterize the transport under voltage and concentration gradient through the membrane first with salt KCl. I-V curves at $pH = 7$ are plotted on Fig. S8(a) for differents $[KCl]$ and we can easily recover the linear response of the current produced by an electric potential drop across the membrane. This allows us to extract the conductance value for each concentration, which is plotted in Fig. S8(b) together with the conduc-

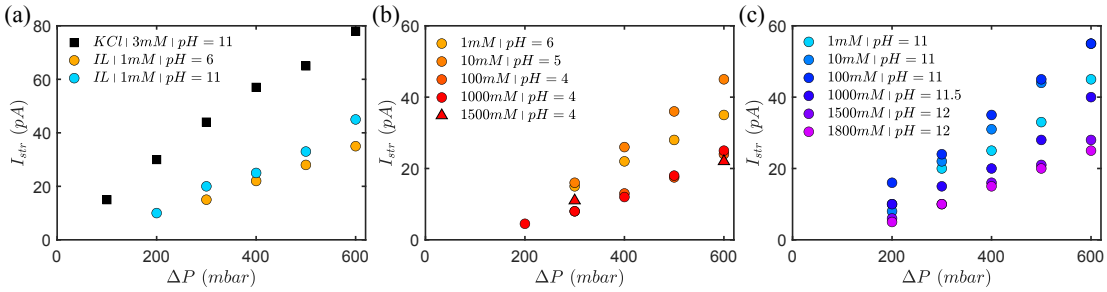

Fig. S 6 (a) Streaming current intensity versus applied pressure for KCl and IL electrolytes in a TiO_2 nanopore. (b)&(c) Similar measurements for IL solutions at pH 5 and 11.

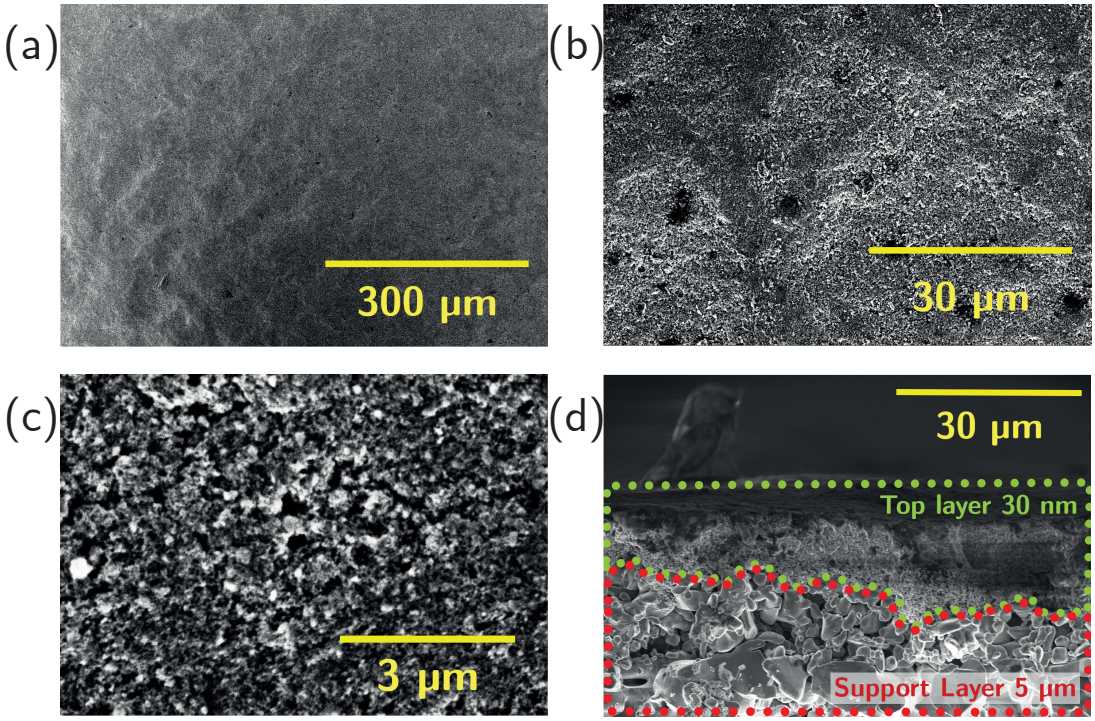

Fig. S 7 SEM images of the macroscopic TiO_2 membrane. (a) Unzoomed view of the surface which shows that on average there are few surface defects. Yellow scale bar corresponds to 300 μm. (b) Intermediate zoomed out view of the surface showing small defects (large black dots) and holes (very small black dots). Yellow scale bar corresponds to 30 μm (c) Close-up view of the surface showing TiO_2 holes (black dots). The average size varies between 30 and 50 nm. The surface density varies between 50 and 100 holes/μm^2. Yellow scale bar corresponds to 3 μm (d) Cross-section of the membrane surface. Inside the green dots is the upper layer with a thickness varying between 5 and 10 μm which is pierced with 30 nm holes as seen in view (c). Inside the red dots are the intermediate granular TiO_2 layers which form paths between the grains and have a size of about 5 μm. Yellow scale bar corresponds to 30 μm.

tance of the cell without the membrane (dotted lines in dark red). A plateau is found at low concentrations, which is consistent with a surface ion transport phenomenon inside the pores. Since we have a macroscopic membrane, in order to extract an order of magnitude of the surface charge inside the pores, we propose the simplest model consisting in considering the membrane as multiple pores gathered in parallel : $G_{membrane} = N * G_{pores}(\Sigma)$. The fit gives $N \approx 4000 - 10000$ pores that corresponds to a surface density of about about $40 - 100$ pores/μm^2 and which is in line with SEM images Fig. S7. This model does not take into account hypothetical interactions that might exist due to the overlapping effects of pore entrance which could affect the pore number exponent N^{β} with β which could be $\neq 1$. This does not prevent the surface charge from being estimated, since it governs the flatness of the curve at low concentrations and not the vertical offset. Surface charge against $[KCl]$ is plotted in Fig. S8(c) which are an order of magnitude lower than those evaluated for a single nanopore of TiO_2 Fig. S4. However, we find the same concentration dependency scale law of $1/3$ like the one for the nanopores.

In a second step, we studied ionic transport under the effect of a salt concentration gradient on both sides of the membrane. For different concentration gradients from 10 to 10^4 we measured the I-V characteristics. The current at zero electrical polarisation $I_{offset(V=0)}$ is the sum of the Nernst current generated by the chemical potential difference of the electrodes due to the different concentrations I_{nernst} and the diffusio-osmotic current $I_{diffusio-osmotic}$. The offset and diffusio-osmotic currents are plotted in Fig. S9(b) and a diffusio-osmotic current of opposite sign to the offset current is observed.

To measure the Nernst potential of Ag/AgCl electrodes in ionic liquids as a function of their concentration, which is not tabulated, we immerse two Ag/AgCl electrodes that constitute the working electrode and the counter electrode as well as a saturated Ag/AgCl reference electrode (PINEresearch LowProfile Reference Electrode). We measure the potential of the working electrode versus the reference electrode in Open Circuit Voltage for each concentration. These measurements are shown in Fig. S10(a). In a second step, we calculate the potential difference corresponding to the gradient we will use, and this gives us the Nernst contribution of the electrodes to the I-V curve measurements shown in Fig. S6 (b) of the main text. Multiplying this by the associated conductance, we have the corresponding Nernst current, and subtracting this from the value of the current for zero potential difference under salt gradient to obtain the diffusio-osmotic current shown in Fig. 6 (b) of the main text.

4 Measurements with $P_{4448}Cl - H_2O$ binary mixture

In parallel to the experiments with $P_{4444}CF_3CO_2 - H_2O$ mixtures, we did similar measurements with another phosphonium-based IL: $P_{4448}Cl$ (this IL does not show an LCST with water but a blend with a more hydrophobic phosphonium IL can lead to the LCST behavior). On Fig. S11(a) are plotted the current intensities I_0 measured at $\Delta V = 0$ for various concentration ratio of $P_{4448}Cl$ and two pH (modulated with HCl and $P_{4448}OH$). As this current is the sum of the Nernst current and the diffusio-osmotic current I_{DO}, the later contribution is isolated using the same reference electrodes as above and plotted on Fig. S11(b). Again, surprisingly, the sign of I_{DO} is negative, underpinning the peculiar interaction of the bulky phosphonium cations with the nanopore surface. There is no great difference observed between the two pH and we notice also that I_{DO} intensity is 3 to 4 times smaller than the intensity collected with KCl solutions for a similar concentration range (see Fig. S5(b)).

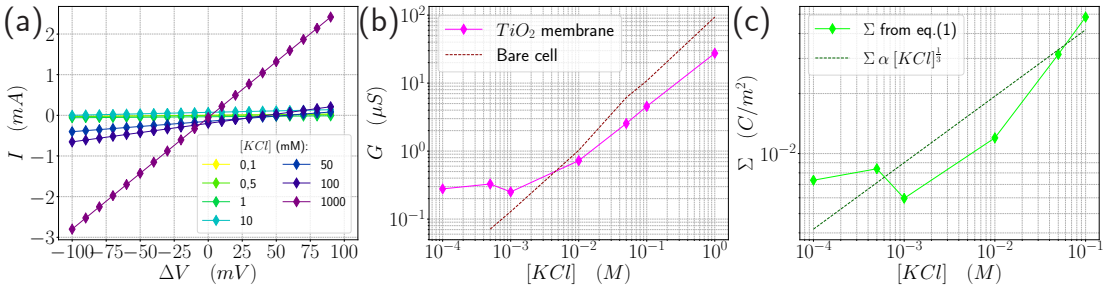

Fig. S 8 (a) I-V curves of the TiO_2 membrane for salt concentration $[KCl]$ varying form $10^{-4}M$ to $1M$ at $pH = 7$. (b) In purple, conductance $G = I/\Delta V$ extracted from (a) and plotted versus the salt concentration $[KCl]$. We note a plateau at the lowest concentration. In darkred dashedlines the conductance of the bare cell without membrane. (C) In green, extracted values of the surface charge obtained by fitting $G_{membrane} = N * G_{pores}(\Sigma)$ with G_{pores} following eq. (1). In darkgreen dashed lines is plotted the model where the surface charge depends on the salt concentration with a exponent $1/3$.

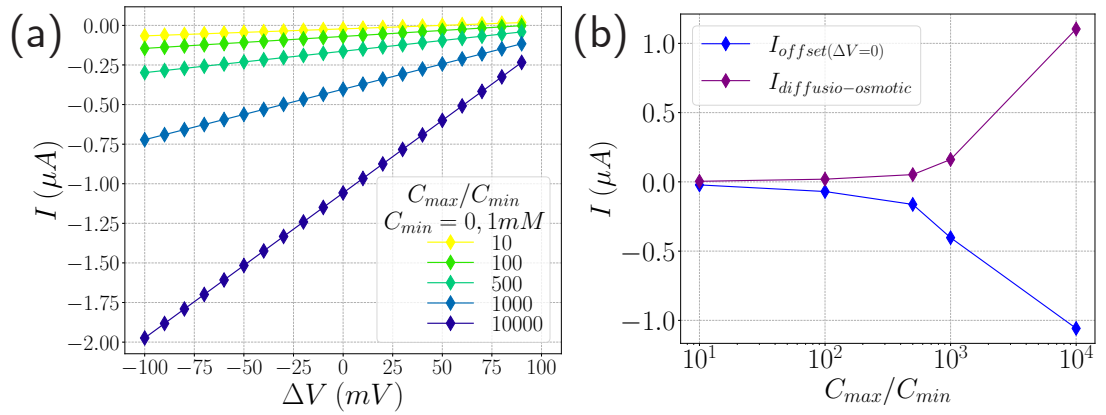

Fig. S 9 (a) I-V curves of the TiO_2 membrane for salt concentration gradient $[KCl]$ varying form 10 to 10^{-4} at $pH = 7$. (b) In blue, the current $I_{offset(V=0)}$ is plotted for zero electrical bias (which corresponds to the y-intercept of the I-V characteristics in Fig. S9 (a)). Purple is the diffusio-osmotic current $I_{diffusio-osmotic}$ obtained by subtracting the Nernst contribution from the zero electric bias current.

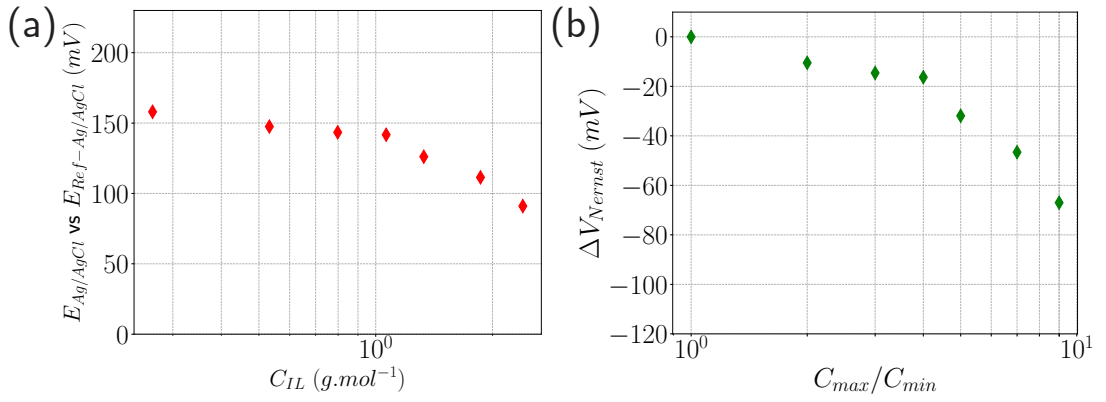

Fig. S 10 Potential of an Ag/AgCl electrode immersed in ionic liquid for various concentrations compared to a reference electrode. (b) Potential difference between two Ag/AgCl electrodes immersed in two different concentrations as a function of this gradient.

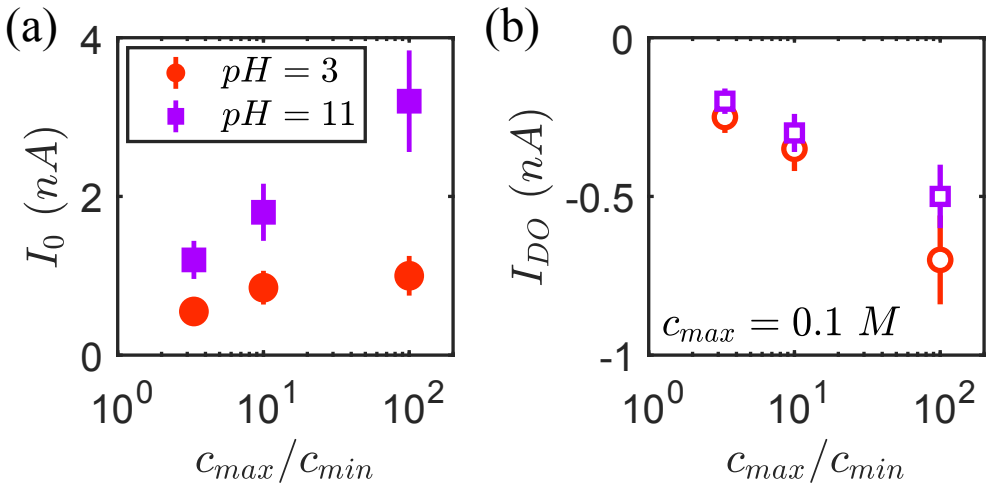

Fig. S 11 (a) Current intensity at $\Delta V = 0$ versus c_{max}/c_{min} for a TiO_2 nanopore submitted to gradients of $P_{4448}Cl$ solutions, at pH 6 and 11. (b) Diffusio-osmotic currents deduced from the values of (a) after substracting the Nernst contribution.